Springer

KSME

Journal of Mechanical Science and Technology 29 (7) (2015) 2987~2993
www.springerlink.com/content/1738-494x(Print)/1976-3824(Online)
DOI 10.1007/s12206-015-0629-5

OWC design to increase wave energy absorption efficiency in wave conversion systems †

Jin-seok Oh* and Jae-hee Jang

Department of Marine Engineering, Korea Maritime and Ocean University, Busan, 606-791, Korea

(Manuscript Received May 9, 2014; Revised March 2, 2015; Accepted March 13, 2015)

Abstract

Oscillating water column (OWC) systems are commonly used as wave energy converters. Such a system consists of an air chamber with a seawater inlet and an air discharger. If seawater moves as a result of the vertical motion of external waves, then the seawater within the OWC moves as well. This movement within the system generates air pressure, which produces power with which to turn the Wells turbine in the air discharge port. OWC systems must be designed in consideration of vibration because waves possess basic oscillation properties. In this research, the efficiency characteristics of OWC systems combined with breakwaters are studied by applying a vibration model. Factors affecting the energy conversion rate of OWC include the volume of air in the air chamber, pressure, and wave period. In this study, changes in the energy absorption efficiency of OWC are measured according to the area ratio between the air discharger and the air chamber, as well as on the basis of air chamber length. Simulations are performed with varying design parameters, such as internal wave, air pressure, and energy, according to changes in external waves. In addition, wave period properties are modified according to the surroundings of the sea in which the OWC system is installed. Variations in these period properties affect energy conversion efficiency. Therefore, changes in energy absorption efficiency due to the wave period are simulated in this study to design an OWC system with high absorption efficiency in view of the characteristic of wave periods in Korea.

Keywords: Conversion efficiency; Oscillating water column (OWC); Wave conversion system; Wave energy

1. Introduction

Interest in renewable energy is currently increasing as a result of environmental issues and high oil prices. Wave power conversion systems are advantageous over their counterparts in that the former can reserve significant amounts of energy and can be designed for small-scale purposes. However, wave power conversions suffer from wave irregularity and low energy efficiency. Nevertheless, studies on the practical use of wave power conversion systems have indicated that the overseas market of wave power generation is established gradually [1]. In particular, hybrid conversion systems for wave power that are coupled with breakwaters can be applied as breakwaters and are durable in long-term use. Among the many existing wave energy converters, oscillating water columns (OWCs) are ideal for application to coasts, especially in Korea. Three sides of this country are surrounded by sea; thus, wave energy is considered an excellent renewable energy source for Korea.

Wave characteristics must be analyzed to determine the energy absorption efficiency of OWC. For instance, McCormick (1981) and Dean (1991) [2, 3] conducted mechanical analyses of waves in their studies. Analytical methods for wave energy converters vary from a simple mass-damping-spring model to computational fluid dynamics model [4, 5]. The design parameters for chamber size and the seawater inlet section are also studied given that these factors influence absorption efficiency. Moreover, air damping on OWC is studied as a factor that influences absorption efficiency. The efficiencies of these design parameters differ depending on the characteristics of waves [6]; thus, the energy efficiency of OWC is investigated in specific sea areas as well [7].

The current study aims to develop a mathematical model to determine the effects of design parameters on the absorption efficiency of a simply designed OWC with a Wells turbine. When seawater motion is induced, the seawater in the OWC moves vertically and air pressure changes. This scenario produces the power with which to turn the Wells turbine in the air discharge port. Then, the tendencies in energy absorption efficiency are studied on the basis of changes in the design parameters. Moreover, the basis of the mass-damping-system model is analyzed in this study. The design of wave power conversion systems is also examined to increase the energy

*Corresponding author. Tel.: +82 51 410 4283
E-mail address: ojs@kmou.ac.kr
† Recommended by Associate Editor Tong Seop Kim

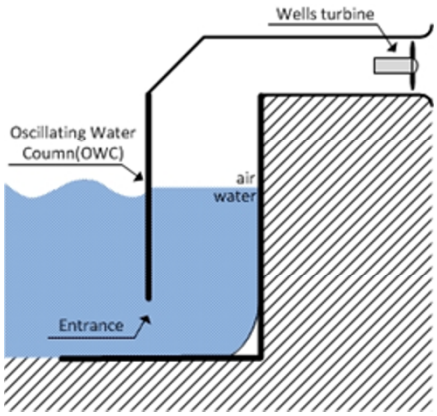

Fig. 1. Schematic of the wave conversion system.

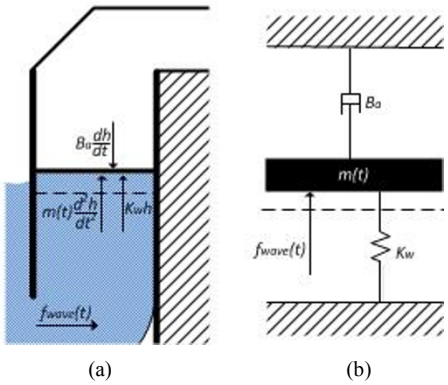

Fig. 2. Vibration model of the wave conversion system.

absorption rate of such systems. Assuming that wave power conversion systems are represented by a vibration model, the model is simulated under several area ratios and air chamber lengths.

2. Modeling of the OWC wave power system

Wave power conversion systems are developed in various forms. In this study, however, the OWC system alone is designed and simulated for application to offshore facilities. This research focuses on the energy conversion efficiency of wave power conversion systems according to the area ratio between the cross-section area of OWC, the area of the air discharger, and OWC length. Fig. 1 presents the schematic of the wave conversion system.

Wave power conversion systems consist of a seawater inlet, OWC, and an air discharger at which the Wells turbine is installed. The hydrostatic pressure generated by external waves exerts a hydrodynamic force on the seawater inlet and induces a reciprocating motion within OWC. This motion facilitates airflow in the air discharger according to the difference in air pressure, and this airflow turns the Wells turbine. This turbine is a widely installed and commonly used wave power converter in OWC; it rotates in only one direction because of its wings, which are installed at 90° in the axial direction of the turbine. Meanwhile, the energy generated by wave power is strongly affected by the internal energy in the OWC system and turbine efficiency.

$$P_{turbine} = \eta \cdot P_{wave} , \tag{1}$$

where P_{wave} is the quantity of energy generated by the waves within the conversion system and η is a factor of energy conversion efficiency in the turbine. Given the system presented in Fig. 1, the vibration model system and the factors that affect it are illustrated in Fig. 2. In this study, energy losses in the inlet and the turbine are not taken into account.

The force that acts at sea level can presumably be represented by a rigid plate within the OWC. Mass changes depending on seawater flow rate. Suppose that the fluid force is excitation force, that the air pressure caused by a decrease in the air discharger denotes damping, and that hydrostatic pressure corresponds to rigidity, the movement of the wave within OWC can be expressed as follows [4]:

$$m(t)\frac{d^2h}{dt^2} + B_a\frac{dh}{dt} + K_w h = f(t) , \tag{2}$$

where *m(t)* is the mass of seawater, which changes depending on inflow and outflow. Thus, the mass of the vibration model varies. The model can be expressed as Eq. (3) by applying Bernoulli equation.

$$m(t) = m_0 + \rho A_b(h_{in} - h_{out}) , \tag{3}$$

where m_0 is the mass of the seawater in the OWC without vibration; v is the specific volume of seawater; ρ is the density; g is the gravitational constant; Δh is the difference in the height of the seawater within and outside of the OWC; and A_b is the cross-sectional area of the OWC chamber.

B_a is the air damping caused by pressure drop due to the change in the area between OWC and the air discharger. This variable can be determined using Eq. (4) [8].

$$B_a = \frac{\Delta p \cdot A_c}{V_c} . \tag{4}$$

$Q = V \cdot A$ where Δp is the air pressure change within the OWC; A_c is the area of the air discharger; and V_c is the air velocity in the air discharger. The area and velocity of each section are indicated in Fig. 3 supposing that A is the seawater inlet, B is the cross section of OWC chamber, and C is the air discharger. Each part can be designed for other areas, and the change in area is expected to affect the variation in fluid velocity from.

The pressure drop in the air chamber can be expressed using the following equations [9, 10]:

$$\Delta p = \frac{\gamma \cdot p_i}{d - h_i(t)} \times h_i(t) , \tag{5}$$

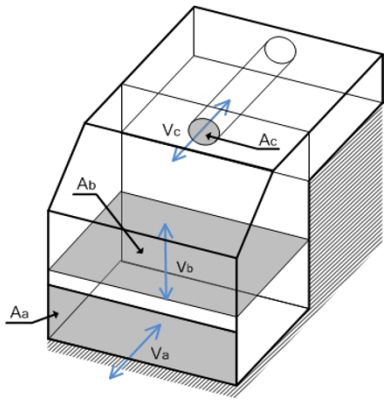

Fig. 3. Area and velocity of each section of the wave power conversion system.

$$p_i = p_o - \frac{1}{2}\rho \cdot V_c^2 \left(1 - \frac{A_c}{A_b}\right), \tag{6}$$

where γ is the specific heat ratio; p_i is air pressure in the air chamber; d is OWC length; $h_i(t)$ is the wave height over time; and V_b is the wave velocity within the OWC.

$$K_w = \rho \cdot g \cdot A_b, \tag{7}$$

$$f(t) = \frac{1}{2} \cdot \rho \cdot C_d \cdot V_a^2(t) \cdot A_a. \tag{8}$$

K_w is the restoring coefficient attributed to hydrostatic pressure and $f(t)$ is the excitation force generated by external waves [11].

$$\omega_r = \omega_n \sqrt{1 - 2\zeta^2}. \tag{9}$$

$$\zeta = \frac{\Delta p \cdot A_c}{2 \cdot V_c \sqrt{(\rho \cdot g \cdot A_b)(m_0 + \rho \cdot A_a \cdot \Delta h)}}. \tag{10}$$

ω_r is the frequency response. Eq. (10) is derived from Eqs. (3), (4), and (7). Therefore, the frequency response increases when air damping is reduced.

3. Simulation

Design parameters affect the energy absorption efficiency of OWC; hence, the thickness of the seawater inlet and the number of chambers have been examined [12, 13]. OWC efficiency and air pressure in the chamber have been studied recently as well [14]. In the present study, I aim to simulate the following design parameters: the ratio of the cross-sectional area and the length of the chamber based on the concept of the mass-damping-spring model.

Given the aforementioned mathematical model, changes in the efficiency of the wave power conversion system can be determined according to the area of the air discharger and OWC length. A_b and A_a, which are the internal cross-sectional area of the OWC and the cross-sectional area of the seawater inlet, respectively, are presumed to be equal to eliminate loss as a result of the change in cross-sectional area and to maintain constant inflow energy.

Table 1. Simulation conditions (1) .

Parameter	Values
Incident wave height (m)	0.13
Wave period (sec)	8
Depth of water (m)	1.7
Width (m)	1.3
Height of OWC (m)	3
	4
	5
Area of water inlet (m^2)	0.65
Area ratio	0.05

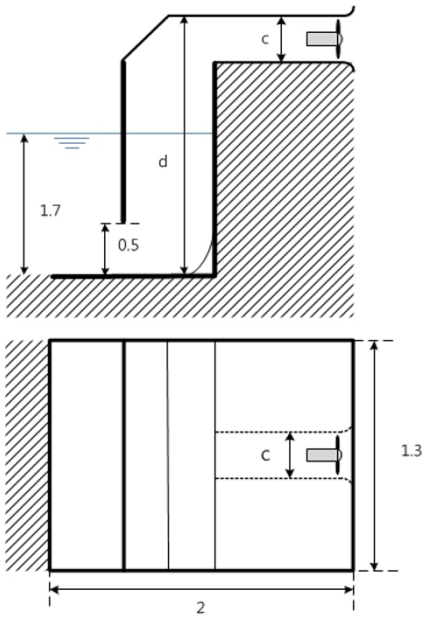

Fig. 4. Size of the simulation model.

The process of altering the energy and height of an internal wave in accordance with OWC length, the area ratio of the air discharger, and the cross section of the OWC is essential in the analysis of physical problems. The size of the wave power conversion system for simulation is presented in Fig. 4.

3.1 Output change in accordance with OWC length

Three conditions are considered in studying the output change that corresponds to OWC length. The simulation duration is 30 seconds, and the other simulation conditions are indicated in Table 1.

The conditions are configured as follows. Case 1: $d = 3$; case 2: $d = 4$; and case 3: $d = 5$. The other conditions are constant. Fig. 5 illustrates the change in OWC wave height in response to the proposed scenario. $h = 0$ corresponds to 1.7 m, which is the height of water without input.

Table 2. Maximum wave height, average wave height, and center of oscillation in each case.

	Case 1	Case 2	Case 3
Max	0.292	0.297	0.300
Mean	0.105	0.106	0.108
Center of oscillation	–0.072	–0.071	–0.070

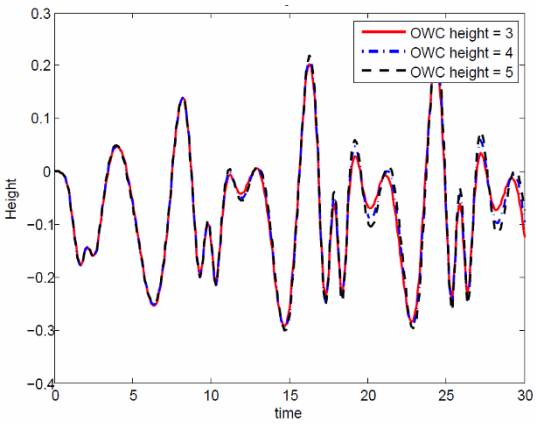

Fig. 5. Change in the internal wave height of OWC in accordance with the conditions of OWC length.

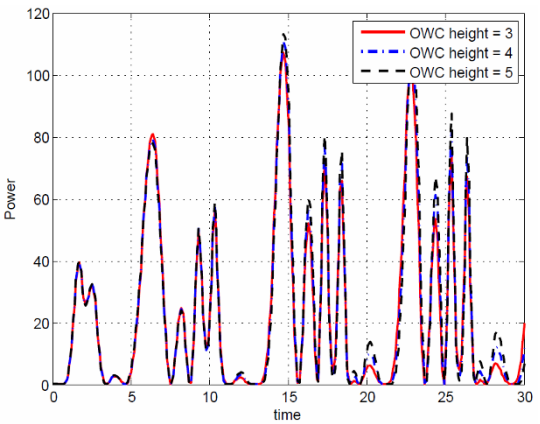

Fig. 6. Change in the internal wave output of OWC in accordance with the conditions of length of OWC.

The amplitude of an internal wave broadens as OWC length increases. Internal waves vibrate more at a lower level than the outside surface of the seawater does as a result of the damping force generated by air [10].

Moreover, the amplitude of the internal wave corresponds to an increase in internal wave energy as a result. Fig. 6 is a time-based graph of the output, which is absorbed by the wave conversion system. Table 3 illustrates the maximum and average outputs.

The difference in the output of the internal wave increases with the difference in internal wave height depending on OWC height. Therefore, the longer the OWC is, the more energy is absorbed because a considerable amount of this energy can be stored as potential energy [10]. As a result, power

Table 3. Maximum and average outputs of each case.

	Case 1	Case 2	Case 3
Max	107.34	110.81	113.05
Mean	22.21	22.84	23.42

Table 4. Simulation conditions (2).

Parameter	Values
Incident wave height (m)	0.13
Wave period (sec)	8
Depth of water (m)	1.7
Width (m)	1.3
Height of OWC (m)	5
Area of water inlet (m^2)	0.65
Area ratio	0.1
	0.05
	0.01

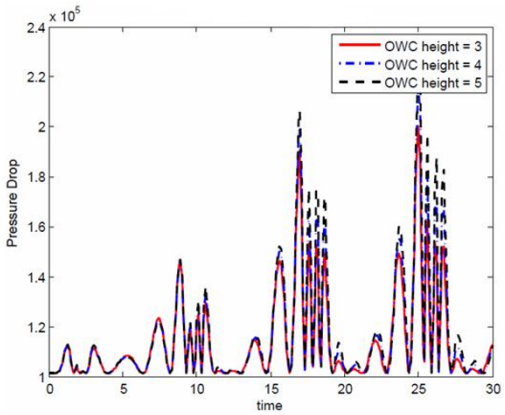

Fig. 7. Change in the air damping of OWC in accordance with the condition of OWC length.

efficiency increases when air damping decreases. Fig. 7 illustrates a change in air damping. When the volume of the air chamber increases, the values of air damping and the difference in damping decrease.

3.2 Output change due to the area ratio of the air discharger

Three conditions are considered in examining the output change corresponding to the area ratio of the air discharger. Simulation duration is 30 seconds, and the other simulation conditions are detailed in Table 4.

Conditions are configured as follows. Case A: $A_c = 0.1$; case B: $A_c = 0.05$; and case 3: $A_c = 0.01$. The other conditions are constant. Fig. 8 is a time-based graph that indicates internal wave height.

The waves in the OWC are highest in case B. On the basis of this simulation result, the height of the internal wave increases as the area ratio decreases. In fact, this height is maximized at approximately $A_c/A_b = 0.05$ before decreasing

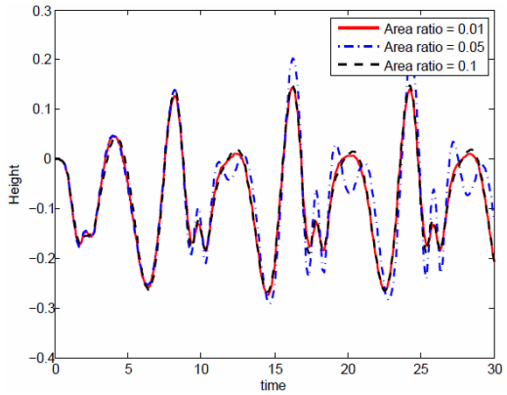

Fig. 8. Change in the internal wave height of OWC in accordance with the condition of OWC area ratio.

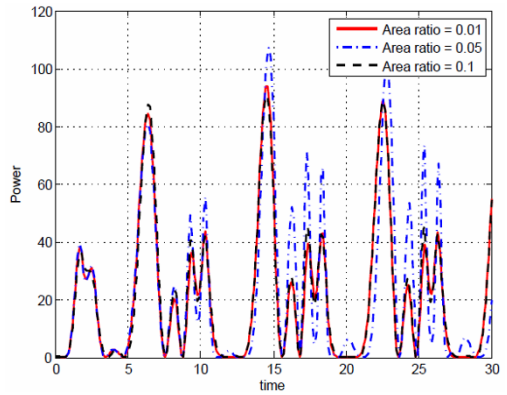

Fig. 9. Change in the internal wave output of OWC in accordance with the condition of OWC area ratio.

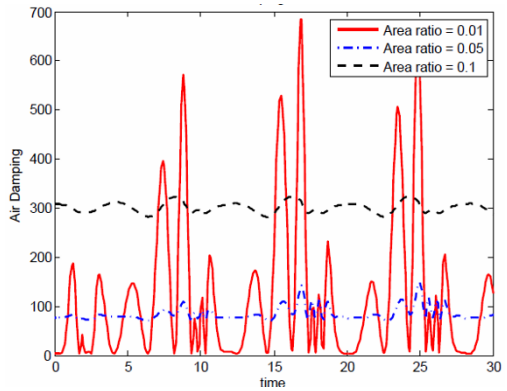

Fig. 10. Change in the air damping of OWC in accordance with the condition of OWC area ratio.

again. This trend is similar to that of wave energy in OWC.

Fig. 9 depicts a graph showing the change in wave energy over time. Case B generates maximum output. The change in air discharger area affects air damping in OWC, thus producing the output presented in the figure. Fig. 10 reveals the simulation result of air damping over time, whereas Table 5 lists the average, maximum, and minimum values of the graph.

As indicated in Fig. 10 and Table 5, the area ratio of the air charger decreases as the difference in air damping increases. The difference in air damping is significant in case C; thus, the average value of air damping in this case is greater than that in case B.

Table 5. Maximum, minimum, and mean air damping of each case.

	Case A	Case B	Case C
Max	684.5	148.3	323.3
Min	2.9	70.0	282.0
Mean	125.1	84.6	301.4

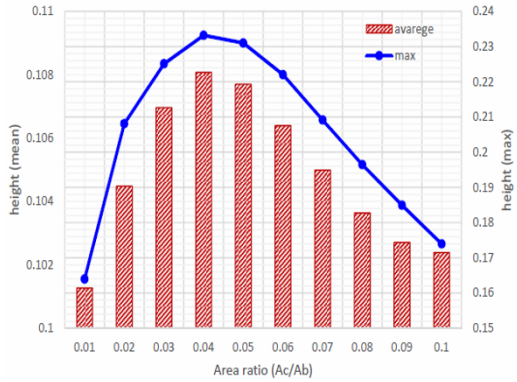

Fig. 11. Average and maximum internal wave heights corresponding to area ratio (with a wave period of eight seconds).

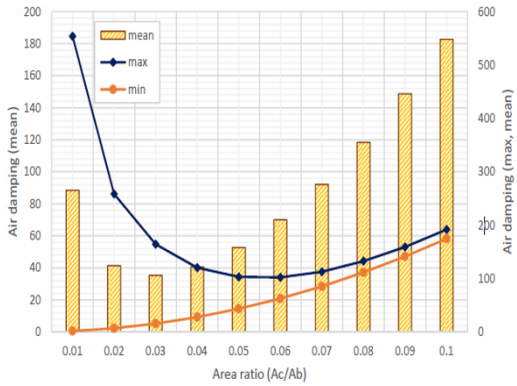

Fig. 12. Average, maximum, and minimum air damping in OWC with respect to area ratio (given a wave period of eight seconds).

4. Analysis of the results

Fig. 11 presents the simulation result that examines how internal wave height can be altered at close to an area ratio of 0.06. With the exception of area ratio, the other simulation conditions are consistent with those shown in Table 3.

The average and maximum values peak when area ratio is 4%. Fig. 12 exhibits a graph illustrating air damping in accordance with area ratio.

When area ratio decreases, the minimum air damping decreases as well. However, the difference between minimum and maximum air damping increases suddenly by less than 0.05. Energy conversion influences both average air pressure

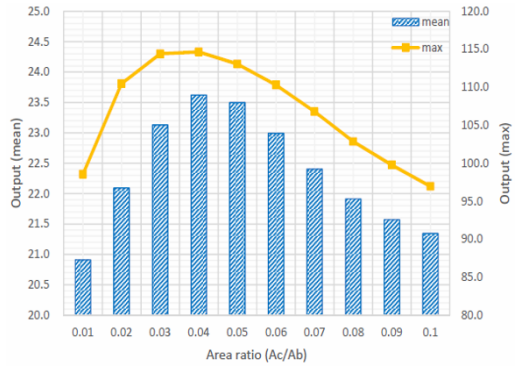

Fig. 13. Average and maximum output in OWC in accordance with area ratio (given a wave period of eight seconds).

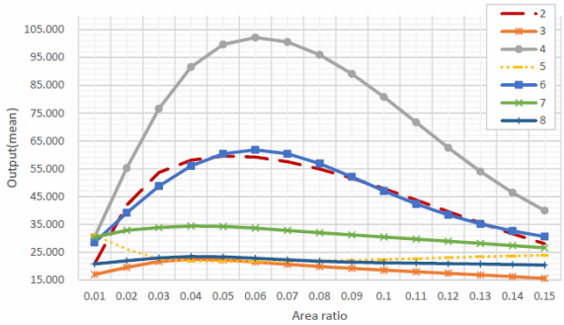

Fig. 14. Average output of each different area ratio due to changes in wave period.

and the difference in air pressure; thus, the conversion is more significant at an air ratio of 0.04 than at an air ratio of 0.03 [8]. Fig. 13 displays a graph showing the output of absorption wave energy in accordance with area ratio.

The graph in Fig. 13 is similar in form to that in Fig. 11. That is, maximum output is also observed at an area ratio of 0.04. The output in OWC affects external wave period as well; therefore, the absorbed energy is related to wave period. The simulated target area ratio is a value between 0.01 and 0.15, and this value results in high output.

Fig. 14 depicts a graph indicating the average output according to area ratio and wave period. This graph also indicates the trend of output according to a wave period of 2–8 seconds and area ratio of 0.01-0.15. Energy is maximized in terms of wave period at the area ratio range of 0.04–0.08 given a wave period of 4 seconds. In Table 6, the maximum values of OWC internal energy are marked in blue. The difference in the output attributed to area ratio can increase significantly from 14% (at a wave period of 8 seconds) to 33% (at a wave period of 4 seconds). The variation in output is determined as per a comparison of maximum output with minimum output. This comparison is highlighted by the following formula:

Maximum and average outputs change irregularly when the wave period is between two and seven seconds. However, output is reduced when the wave period exceeds seven seconds.

Fig. 15 shows the graph indicating the maximum and minimum outputs, as well as the mean outputs.

Table 6. Average output of each different area ratio due to changes in wave period.

		Area ratio						
		0.03	0.04	0.05	0.06	0.07	0.08	0.09
Wave period	2	53.70	58.09	**59.57**	59.22	57.56	54.95	**51.67**
	3	21.74	**22.58**	22.32	21.56	20.71	19.94	**19.27**
	4	**76.58**	91.55	99.63	**102.14**	100.55	95.94	89.10
	5	**22.68**	21.88	**21.77**	21.78	21.84	21.94	22.13
	6	**48.78**	56.04	60.42	**61.80**	60.42	56.90	52.13
	7	33.92	**34.45**	34.32	33.71	32.91	32.08	**31.29**
	8	23.05	**23.54**	23.42	22.92	22.33	21.84	**21.50**

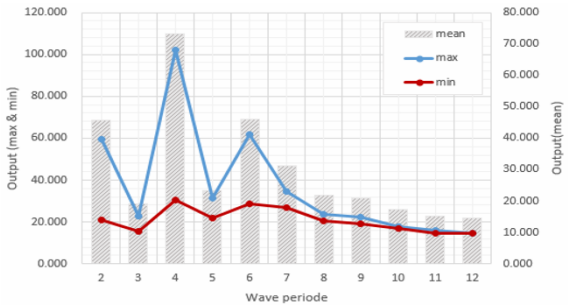

Fig. 15. Maximum outputs, minimum outputs, and average outputs corresponding to wave periods (including all area ratios).

$$\Delta\eta_{area} = \frac{P_{\max} - P_{\min}}{P_{\min}}. \tag{11}$$

Given that the significant wave period of Korea lasts for eight seconds, an area ratio of 0.04 is expected to be appropriate for the installation of an OWC system in Korea. Nevertheless, the characteristics of sea areas in Korea should be investigated for designing an optimized wave conversion system [15].

5. Conclusions

In this study, the wave conversion system that includes OWC is presumably represented by a vibration model. This system is simulated based on OWC length and the area ratio of the air discharger. First, internal wave energy increases as OWC length increases because the air volume can prevent an increase in energy. Second, the output of OWC is highest at an area ratio of 0.06. Thus, the average ratio of energy absorption is obtained when the wave period is between two and eight seconds.

The area ratio of maximum energy absorption efficiency varies slightly depending on wave period. Therefore, the characteristics of wave design location are crucial to OWC design. Nonetheless, the area ratio of 0.04 is more appropriate for the installation of wave conversion systems in the sea areas of Korea because the average specific wave period in this country is usually eight seconds long.

Acknowledgement

This work was supported by the World Class 300 R&D Program (10050317, Development of eco-friendly Single Point Mooring System with integrated control system operable up to maximum water depth 100 meters) funded by the Small and Medium Business Administration (SNBA, Korea).

Nomenclature

A_a : Area of Section A (m^2)
A_b : Area of Section B (m^2)
A_c : Area of Section C (m^2)
B_a : Air damping (kg/s)
C_d : Coefficient of resistance that depends on Reynolds number
D : Length of OWC (m)
F : Excitation force (force of external wave, kg · m/s^2)
h_i : Wave height of OWC (m)
h_o : Wave height of external wave (m)
K_w : Rigidity (hydrostatic pressure, kg/s^2)
M : Mass of water in OWC (kg)
m_0 : Initial mass of water in OWC (kg)
$P_{turbine}$: Output of turbine (kg · m^2/s^3)
P_{wave} : Output of internal wave of OWC (kg · m^2/s^3)
P_{ma} : Maximum output (kgm^2/s^3)
P_{min} : Minimum output (kg · m^2/s^3)
Δp : Pressure drop (kgf/cm^2)
V_b : Velocity of sea surface in OWC at Section B (m/s)
V_c : Velocity of air at Section C (m/s)
H : Conversion efficiency of turbine
$\Delta\eta_{area}$: Difference of output efficiency
N : Specific volume of seawater (m^3/kg)
γ : Specific heat ratio

References

[1] C. H. Shin and K. Y. Hong, The State-of-the-art and performance indicators for commercial use of the wave energy utilization technologies, *Journal of Korea Society of Civil Engineers*, 59 (5) (2011) 55-62.
[2] M. E. McCormick, *Ocean wave energy conversion*, Dover Publication, Inc., Minelola, New York, USA (1981).
[3] R. G. Dean and R. A. Dalrymple, *Water wave mechanics for engineers and scientists*, World Scientific Publishing Co. Pte. Ltd., USA (1991).
[4] V. Karami, M. J. Ketabdari and A. K. Akhtari, Numerical modeling of oscillating water column wave energy convertor, *Journal of Advanced Renewable Energy Research*, 4 (1) (2012) 196-206.
[5] A. E. Marhani, F. Castro, M. Bahaji and B. Filali, 3D unsteady flow simulation in an owc wave converter plant, *ICREPQ*, 6 (2006) 5-7.
[6] Y. Luo, J. R. Nader, P. Cooper and S. P. Zhu, Nonlinear 2D analysis of the efficiency of fixed oscillating water column wave energy converters, *Journal of Renewable Energy*, 64 (2013) 255-265.
[7] M. F. Hsieh, I. H. Lin, D. G. Dorrell, M. J. Hsieh and C. C. Lin, Development of a wave energy converter using a two chamber oscillating water column, *Sustainable Energy, IEEE Transactions on*, 3 (3) (2012) 482-497.
[8] R. Curran, Ocean wave energy systems design: Conceptual design methodology for the operational matching of the wells air turbine, *Collaborative Product and Service Life Cycle Management for a Sustainable World* (2008) 601-615.
[9] W. Sheng, T. Lewis and R. Alcorn, On wave energy extraction of oscillating water column device, *Proc. of 4th International Conference on Ocean Energy* (2012) 1-9.
[10] I. G. Morrison and C. A. Greated, Oscillating water column modelling, *Proc. of 23rd Conference on Coastal Engineering* (1992) 502-511.
[11] M. Karlsteen, *The dynamic mooring force on a wave energy converter moored in a single point*, Chalmers University of Technology, Gothenburg, Sweden (2012).
[12] D. G. Dorrell and M. F. Hsieh, Performance of wells turbines for use in small-scale oscillating water columns, *Proc. of 18th International Offshore and Polar Engineering Conference* (2008) 393-400.
[13] B. Bouali and S. Larbi, Contribution to the geometry optimization of an oscillating water column wave energy converter, *Energy Procedia*, 36 (2013) 565-573.
[14] I. Lopez, B. Pereiras, F. Castro and G. Iglesias, Optimisation of the turbine-induced damping for an OWC wave energy converter using a RANS-VOF numerical model, *Journal of Applied Energy*, 127 (2014) 105-114.
[15] C. G. Kim, Y. D. Choi, Y. H. Hwang and Y. H. Lee, Effect of wave conditions on the performance of a direct drive turbine, *Proc. Korea Society of Mechanical Engineers* (2009) 90-91.

Jin Seok Oh received his B.E. in Marine Engineering from Korea Maritime and Ocean University, Pusan, Korea, in 1983. He obtained his M.S. and Ph.D. in Electric Control Engineering from Korea Maritime and Ocean University, Pusan, Korea, in 1989 and 1996, respectively. He obtained another Ph.D. degree in Design of Energy from Kyushu University, Kyushu, Japan, in 2009. From 2001 to 2006, he was employed as an energy and automation consultant in U.K. K.O. Tech. He has worked as a professor since 1996. His current research interests include ocean plants, renewable energy, and design of energy.

Jae Hee Jang received her B.E. in Mechanical Engineering from Kumoh National Institute of Technology in 2013. She is pursuing her Master's degree in the Department of Marine Engineering, Korea Maritime and Ocean University.